Tailoring magnetic orders in $(LaFeO_3)_n$–$(LaCrO_3)_n$ superlattices model

Yangyang Zhu,[1] Shuai Dong,[1,2,a)] Qinfang Zhang,[3,4] Seiji Yunoki,[3,4,5] Yonggang Wang,[1] and J.-M. Liu[2,6]
[1]*Department of Physics, Southeast University, Nanjing 211189, China*
[2]*Labotatory of Solid State Microstructures, Nanjing University, Nanjing 210093, China*
[3]*Computational Condensed Matter Physics Laboratory, RIKEN ASI, Wako, Saitama 351-0198, Japan*
[4]*CREST, Japan Science and Technology Agency (JST), Kawaguchi, Saitama 332-0012, Japan*
[5]*Computational Materials Science Research Team, RIKEN AICS, Kobe, Hyogo 650-0047, Japan*
[6]*International Center for Materials Physics, Chinese Academy of Sciences, Shenyang 110016, China*

(Received 25 June 2011; accepted 29 July 2011; published online 14 September 2011)

Magnetic orders in $(LaFeO_3)_n$–$(LaCrO_3)_n$ superlattices and in the corresponding $LaFe_{0.5}Cr_{0.5}O_3$ are studied by Monte Carlo simulations. Because of the different exchange couplings of Fe–O–Fe, Cr–O–Cr, and Fe–O–Cr, the superlattices show nontrivial magnetic modulations with the stack periods. Our simulations not only reproduce the experimental observation of strong ferromagnetism in the $n = 1$ superlattice, but also predict other complex antiferromagnetic or ferrimagnetic orders in thicker cases. The possible chemical phase separation in $LaFe_{0.5}Cr_{0.5}O_3$ bulk is also revealed in our simulation. © *2011 American Institute of Physics*. [doi:10.1063/1.3631787]

INTRODUCTION

Oxides are usually strongly correlated electronic materials, which host many emergent physical properties, such as the high-T_c superconducting and colossal magnetoresistivity.[1] In recent years, oxide heterostructures attracted many research interests because of their potential applications as new electronic devices.[2] For example, the conducting two-dimensional (2D) electronic gas was found at the interfaces between insulating perovskites.[3] By using the digital-synthesis techniques, manganite superlattices (SLs) were fabricated with atomic-scale smooth interfaces, which showed many fascinating properties, e.g., the metal-insulating transition[4] and enhancement of A-type antiferromagnetic (A-AFM) ordering.[5] Accompanying these advanced experimental investigations, theoretical studies have tried to reveal the physical mechanisms behind these phenomena. In these oxide heterostructures, the key physical issue is "reconstructions": not only the electronic reconstruction induced by charge leakage, but also the lattice reconstruction imposed by strain/stress.[6] These reconstructions can change the physical properties (including magnetism, charge, orbits, conductivity, etc.) of heterostructures from their corresponding bulks.

Among these changes, the modulation of magnetism, including magnetic phase transitions and magnetic couplings, is very attractive in oxide heterostructures. For example, a strong magnetization was found in $LaMnO_3/SrMnO_3$ SLs, although both of these manganites are antiferromagnetic (AFM) in bulk.[4] In contrast, an AFM coupling was discovered between $La_{0.7}Sr_{0.3}MnO_3$ and $SrRuO_3$ interfaces,[7] while both compounds are themselves strongly ferromagnetic (FM). And electric-controllable exchange bias was found in $La_{0.7}Sr_{0.3}MnO_3/BiFeO_3$ heterostructures, although $BiFeO_3$ is a G-type antiferromagnetic (G-AFM) multiferroic material.[8] The modulation of magnetism widely exists in various oxides heterostructures.

For instance, both the ground states of $LaFeO_3$ and $LaCrO_3$ are G-AFM materials in bulk, and the Néel temperatures (T_Ns) are 750 K and 280 K, respectively.[9] However, ferromagnetism (or ferrimagnetism) was realized in the $LaCrO_3$–$LaFeO_3$ SLs by stacking Cr^{3+} and Fe^{3+} one by one along the [111] direction.[9] The Curie temperature (T_C) of this FM $LaCrO_3$–$LaFeO_3$ SLs is about 375 K, and its saturated magnetization approaches 3 μ_B per site.[9] In addition, by changing the deposition directions, Ueda *et al.*[9] also achieved more magnetic orders in these $LaCrO_3$–$LaFeO_3$ superstructures, e.g., A-AFM one on $SrTiO_3$ (110) and C-type antiferromagnetic (C-AFM) one on $SrTiO_3$ (100).[10] In contrast, the $LaCr_{1/2}Fe_{1/2}O_3$ thin film shows an paramagnetic–-antiferromagnetic transition at 320 K,[9] which may be phase separated into Fe^{3+}-rich and Cr^{3+}-rich regions.[11]

The physical mechanism beyond these magnetic modulations is the diverse couplings of Fe–O–Fe, Cr–O–Cr, and Fe–O–Cr bonds. Unlike the AFM Fe–O–Fe and Cr–O–Cr interactions, a FM coupling is formed within the Fe–O–Cr bond.[9–11] Therefore, the magnetic orders in $LaCrO_3/LaFeO_3$ heterostructures and bulks can be modified by different Fe/Cr distributions at the interfaces. Thus, it is straightforward to understand the FM, A-AFM, and C-AFM states in above $LaCrO_3/LaFeO_3$ SLs grown along different axes.

In this paper, we performed Monte Carlo (MC) simulations on a simple model for $LaCrO_3/LaFeO_3$ SLs. More complex spin structures besides the aforementioned three states have been predicted by adopting different Fe/Cr distributions.

MODELS AND METHODS

To simulate the $LaCrO_3/LaFeO_3$ SLs and bulk, 2D spin lattices (square $L \times L$, $L = 48$) are studied. For SLs, the Fe and Cr layers are deposited alternatively along the diagonal direction (the [11] axis in 2D lattice).[11] The thicknesses of each Fe layer and Cr layer are equal and can be modulated in our simulations, e.g., SL(n) denotes $(LaFeO_3)_n$–$(LaCrO_3)_n$.

a)Author to whom correspondence should be addressed. Electronic mail: sdong@seu.edu.cn.

For comparison, the bulk is also simulated by distributing Fe/Cr cations randomly. In all our simulations, the ratio between Fe and Cr is 1:1.

The XY spin model is adopted here, and the Hamiltonian can be written as:

$$H = \sum_{<i,j>} J_{ij} S_i \cdot S_j + h \sum_i S_i, \quad (1)$$

where J_{ij} is the interaction between the nearest-neighbor spins S_i and S_j (i and j are site indexes); h is the magnetic field applied along x direction, and the normalization $|S| = 1$ will be used in the following. Moreover, the XY-type spins are suitable to simulate the magnetic anisotropy (easy-plane) in real SLs grown on substrates where their magnetic moments are almost in-plane.[9,10]

In the following simulations, three exchange interactions (J_{FF}, J_{CC}, and J_{FC}) are used to simulate the couplings between Fe–O–Fe, Cr–O–Cr, and Fe–O–Cr, respectively. The values of exchange interactions are chosen to be $J_{FF} = 7.5$, $J_{CC} = 2.8$, and $J_{FC} = -3.7$ considering the T_Ns of $LaFeO_3$ and $LaCrO_3$ and T_C of $LaFeO_3$–$LaCrO_3$ [111] superlattice. A tiny magnetic field $h = 0.1$ is applied to measure magnetizations in all simulations.

The standard Markov chain Monte Carlo (MC) method is employed in our simulations. Typically 2×10^4 MC steps are used for thermal equilibrium and the following 4×10^4 MC steps are used for measurements. The updates of spins are determined by the standard Metropolis algorithm, and the acceptance ratio is controlled to be about 50% at low temperatures (Ts) by adjusting the updating spin windows.

To trace magnetic phase transitions, the total energies, specific heats, and magnetizations are measured as a function of T. To distinguish various AFM spin structures, the spin structure factors are also calculated as[12]:

$$S(k) = \sum_{i,r} S_i \cdot S_{i+r} \cos(2\pi k \cdot r), \quad (2)$$

where $\boldsymbol{r}$ and $\boldsymbol{k}$ are vectors in real and reciprocal spaces, respectively. Typically, different magnetic orders correspond to different peak positions in the reciprocal space.

RESULTS AND DISCUSSION

Figure 1(a) shows T-dependence of (MC-averaged) energies per site ($\langle E \rangle$, where $\langle\rangle$ denotes the MC average) in the $LaFeO_3$–$LaCrO_3$ SLs. Among all simulated structures, the energy of SL(1) is the highest in the whole temperature region. With the increasing n, the system energy decreases gradually. The energies of SL(3) and SL(4) are already very close, especially in the low-temperature region.

For comparison, the bulk system is simulated with random distributions of Cr and Fe sites. Different random configurations have been tested and the energy-versus-temperature curves are quite similar. The bulk's energy, as shown in Fig. 1(a), is lower than the one of SL(1) but higher than the ones of SL(3) and SL(4). According to the exchange energy, the random configuration of Cr and Fe in $LaFe_{0.5}Cr_{0.5}O_3$ bulk is unstable against the phase separation into $LaFeO_3$ and $LaCrO_3$ clusters. Therefore, intrinsic inhomogeneity may emerge in $LaFe_{0.5}Cr_{0.5}O_3$ bulk, as observed experimentally.[9,11] Also, the SL(1) and SL(2) should be metastable configurations because their exchange energies are notably higher than SL(4). Thus, such thin SLs cannot be obtained in the conventional bulk phase, and can only be stacked artificially by using the pulsed laser deposition. Of course, in real materials, other energy items, especially those concerning the lattice distortions, should also be taken into account when deciding whether the system is phase separated or homogeneous. Even though, according to our simulation, a phase separation tendency is expected from the aspect of exchange interactions.

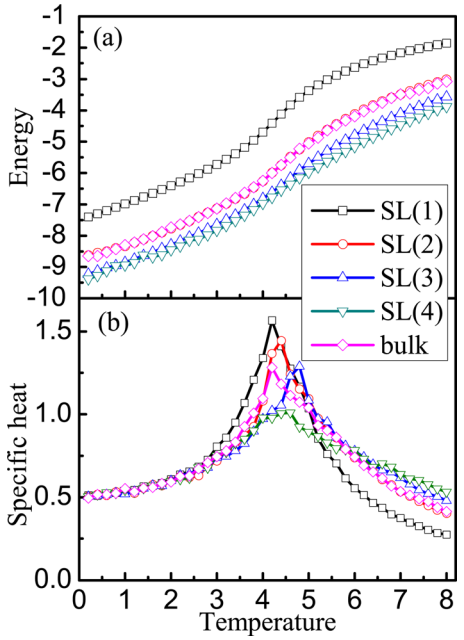

FIG. 1. (Color online) (a) Temperature dependence of energies in $LaFeO_3$–$LaCrO_3$ SLs. The bulk is simulated with a random-mixed distribution of Fe and Cr sites. (b) The corresponding specific heats.

The specific heat $C(T)$ per site of the $LaFeO_3$–$LaCrO_3$ SLs and bulk is also calculated by the standard fluctuation equation ($C(T) = N(\langle E^2 \rangle - \langle E \rangle^2)/k_B T^2$, here the Boltzmann constant k_B is taken as 1 and N is the number of total sites), as shown in Fig. 1(b). All $C(T)$ curves show peaks around 4–5, suggesting phase transitions at similar temperatures. The T_C of SL(1) is lower than the T_Ns of thicker SLs in our simulations, in agreement with the experimental observation.[10] However, the bulk's transition temperature here is close to that of SL(1), which disagrees with the experimental data.[9] This disagreement also implies that the distribution of Fe and Cr cations may be non-uniform; namely, the real $LaFe_{0.5}$ $Cr_{0.5}O_3$ may be phase separated.

The magnetizations (Ms) of $LaFeO_3$–$LaCrO_3$ SLs are obtained under a weak magnetic field ($h = 0.1$, along x direction), as shown in Fig. 2. Strong FM signals have been observed in both the SL(1) and SL(3), and the T_Cs are about 4.5, in agreement with previous specific heats' behavior. The magnetic moment in SL(1) can be totally saturated at low temperatures, namely all spins are parallel. In contrast, the maximum M of SL(3) is only about 1/3. Therefore, the magnetic order in SL(3) may be ferrimagnetic, which will be further clarified in the

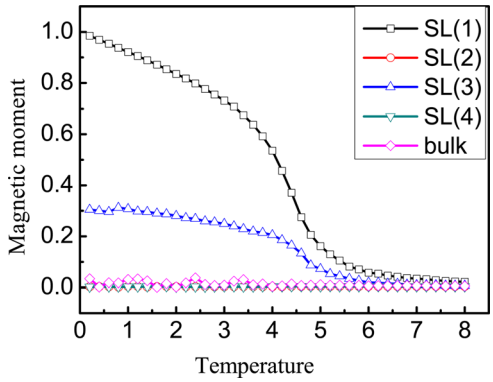

FIG. 2. (Color online) Temperature dependence of magnetizations in $LaFeO_3$–$LaCrO_3$ SLs. Only the SL(1) and SL(3) show significant magnetizations.

following. The *Ms* of SL(2), SL(4), and bulk are much weaker (almost zero), suggesting possible AFM states at low *T*s.

To identify the microscopic magnetic orders in these SLs and bulk, the low-*T* ($T=0.2$) spin structure factors are calculated and shown in Fig. 3. For the SL(1), only a sharp peak appears at $k=(0, 0)$ (the Γ point), which is a definitive proof of FM order. For the SL(2), two equivalent peaks appear at $k=(\pi/2, 3\pi/2)$ and $(3\pi/2, \pi/2)$ along the diagonal line of the Brillouin zone (BZ), which suggests a possible E-type antiferromagnet. Three peaks appear in the SL(3) case: two equivalent strong peaks at $k=(2\pi/3, 4\pi/3)$ and $(4\pi/3, 2\pi/3)$ and a weak peak at the Γ point. The height of Γ point peak is about 1/4 of one main peak and thus 1/9 of all peaks. Because the spin structure factor at the Γ point is in fact the average of M^2, its value ($\approx 1/9$) coincides with the saturated M ($\approx 1/3$) in SL(3) very well, suggesting a ferrimagnetic order. The SL(4) case is more complex: two weak ones

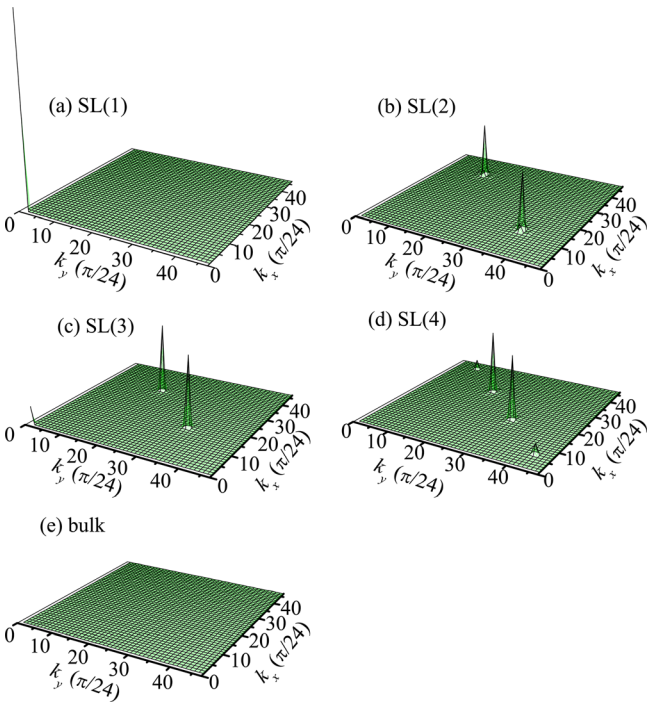

FIG. 3. (Color online) Low-*T* spin structure factors: (a–d) $LaFeO_3$–$LaCrO_3$ SLs; (e) alloy-mixed bulk. The z-axes are in the same scale, so the height of peaks can be compared directly.

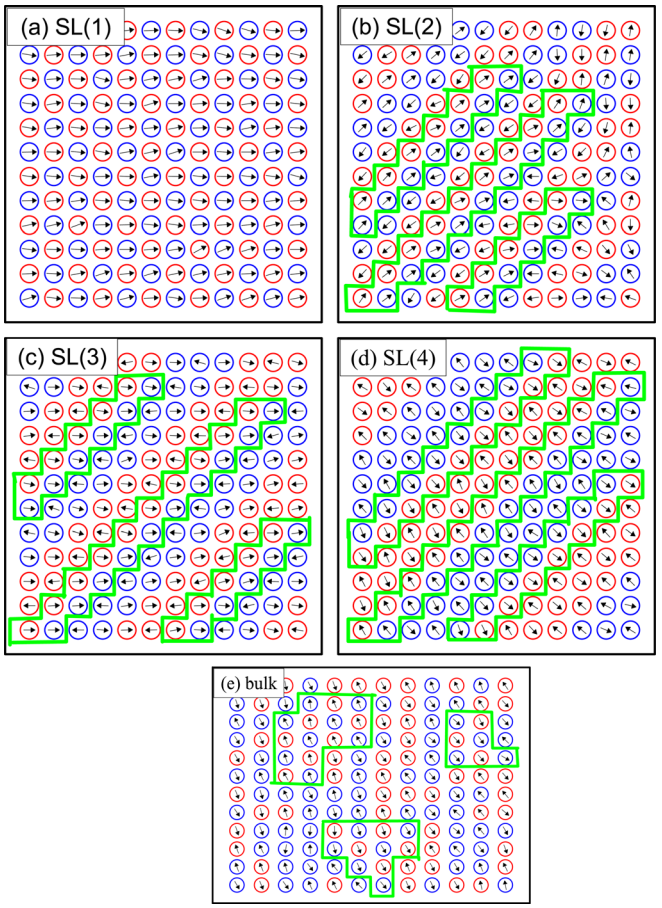

FIG. 4. (Color online) Low-*T* MC snapshots of spin patterns: (a–d) $LaFeO_3$–$LaCrO_3$ SLs; (e) alloy-mixed bulk. Only 12×12 sublattices are shown here. The arrows represent the spin vectors. The red (blue) circles denote the Fe (Cr) sites. Some local FM regions are highlighted by green frames.

at $(\pi/4, 7\pi/4)$ and $(7\pi/4, \pi/4)$, two strong ones at $(3\pi/4, 5\pi/4)$ and $(5\pi/4, 3\pi/4)$, and the height ratio is about 5.8. In contrast, the spin structure factor of bulk sample does not show any clear peaks even at this low-*T*, as shown in Fig. 3(e). This chaotic profile of spin structure factor implies the absence of any long-range orders in the alloy-mixed bulk, which is different from the real material that shows an AFM transition at 320 K. Therefore, the spin structure factor also suggests a chemical phase separation in real material.

To better view the magnetic orders of these heterostructures, the low-*T* ($T=0.2$) MC snapshots of spin patterns in these SLs are shown in Fig. 4. The local FM orders are marked with green frames. For SL(1) (Fig. 4(a)), all spins are almost parallel, suggesting the FM magnetic order, The tiny canting angles of spins are because of the thermal fluctuation of MC simulation. In other SLs (Fig 4. (b–d)), FM and AFM orders are modulated with the periods of the SLs. These special FM/AFM modulations give rise to the spin structure factors shown in Fig. 3. Regarding the alloy-mixed bulk, any long-range spin order is absent, but some short-range FM or AFM clusters persist.

CONCLUSION

In summary, a simple spin model for $LaFeO_3$–$LaCrO_3$ SLs has been simulated by the MC method. The key physical issue is the FM coupling mediated by the Fe–O–Cr bond and

the AFM couplings between Fe–O–Fe and Cr–O–Cr themselves. The total magnetizations of SLs depend on the cation orders at the interface. The FM and ferrimagnetic behaviors are obtained in SL(1) and SL(3), while two different AFM orders have been observed in SL(2) and SL(4). Our results not only support the experimental data in the SL(1) but also predict new possible ordered phases in these SLs with other periods. In contrast, the alloy-mixed bulk does not show a long-range magnetic order in our simulation. The divergence between our simulation and experimental results suggests a possible chemical phase separation in real $LaFe_{0.5}Cr_{0.5}O_3$.

ACKNOWLEDGMENTS

This work is supported by the 973 Projects of China (2011CB922101, 2009CB623303), NSFC (11004027), and NCET (10-0325).

[1]E. Dagotto, Science **309**, 262 (2005).
[2]E. Dagotto, Science **318**, 1076 (2007); H. Takagi and H. Y. Hwang, *ibid.* **327**, 1601 (2010); J. Mannhart and D. G. Schlom, *ibid.* **327**, 1607 (2010).
[3]A. Ohtomo, D. A. Muller, J. L. Grazul, and H. Y. Hwang, Nature (London) **419**, 378 (2002); A. Ohtomo and H. Y. Hwang, *ibid.* **427**, 423 (2004); S. Thiel, G. Hammerl, A. Schmehl, C. W. Schneider, and J. Mannhart, Science, **313**, 1942 (2006).
[4]A. Bhattacharya, S. J. May, S. G. E. te Velthuis, M. Warusawithana, X. Zhai, B. Jiang, J.-M. Zuo, M. R. Fitzsimmons, S. D. Bader, and J. N. Eckstein, Phys. Rev. Lett. **100**, 257203 (2008).
[5]S. J. May, P. J. Ryan, J. L. Robertson, J.-W. Kim, T. S. Santos, E. Karapetrova, J. L. Zarestky, X. Zhai, S. G. E. te Velthuis, J. N. Eckstein, S. D. Bader, and A. Bhattacharya, Nature Mater. **8**, 892 (2009).
[6]S. Okamoto and A. J. Millis, Nature (London) **428**, 630 (2004); S. Dong, R. Yu, S. Yunoki, G. Alvarez, J.-M. Liu, and E. Dagotto, Phys. Rev. B **78**, 201102(R) (2008).
[7]M. Ziese, I. Vrejoiu, E. Pippel, P. Esquinazi, and D. Hesse, Phys. Rev. Lett. **104**, 167203 (2010); M. Ziese, I. Vrejoiu, and D. Hesse, Appl. Phys. Lett. **97**, 052504 (2010).
[8]S. W. Wu, S. A. Cybart, P. Yu, M. D. Rossell, J. X. Zhang, R. Ramesh, and R. C. Dynes, Nature Mater. **9**, 756 (2010); S. Dong, K. Yamauchi, S. Yunoki, R. Yu, S. Liang, A. Moreo, J.-M. Liu, S. Picozzi, and E. Dagotto, Phys. Rev. Lett. **103**, 127201 (2009).
[9]K. Ueda, H. Tabata, and T. Kawai, Science **280**, 1064 (1998).
[10]K. Ueda, H. Tabata, and T. Kawai, J. Appl. Phys. **89**, 2847 (2001).
[11]Y Ijiri, J. Phys.: Condens. Matter **14**, R947 (2002).
[12]S. Dong, R. Yu, S. Yunoki, J.-M. Liu, and E. Dagotto, Phys. Rev. B **78**, 064414 (2008).